

Studies in Systems, Decision and Control

Volume 434

Series Editor

Janusz Kacprzyk, Systems Research Institute, Polish Academy of Sciences,
Warsaw, Poland

The series “Studies in Systems, Decision and Control” (SSDC) covers both new developments and advances, as well as the state of the art, in the various areas of broadly perceived systems, decision making and control—quickly, up to date and with a high quality. The intent is to cover the theory, applications, and perspectives on the state of the art and future developments relevant to systems, decision making, control, complex processes and related areas, as embedded in the fields of engineering, computer science, physics, economics, social and life sciences, as well as the paradigms and methodologies behind them. The series contains monographs, textbooks, lecture notes and edited volumes in systems, decision making and control spanning the areas of Cyber-Physical Systems, Autonomous Systems, Sensor Networks, Control Systems, Energy Systems, Automotive Systems, Biological Systems, Vehicular Networking and Connected Vehicles, Aerospace Systems, Automation, Manufacturing, Smart Grids, Nonlinear Systems, Power Systems, Robotics, Social Systems, Economic Systems and other. Of particular value to both the contributors and the readership are the short publication timeframe and the world-wide distribution and exposure which enable both a wide and rapid dissemination of research output.

Indexed by SCOPUS, DBLP, WTI Frankfurt eG, zbMATH, SCImago.

All books published in the series are submitted for consideration in Web of Science.

More information about this series at <https://link.springer.com/bookseries/13304>

Moussa Labbadi · Kamal Elyaalaoui ·
Loubna Bousselamti · Mohammed Ouassaid ·
Mohamed Cherkaoui

Modeling, Optimization and Intelligent Control Techniques in Renewable Energy Systems


An Optimal Integration Of Renewable Energy
Resources Into Grid

Moussa Labbadi
INSA Hauts-de-France
Université Polytechnique Hauts-de-France
Valenciennes, France

Loubna Bousselamti
Mohammed V University in Rabat
Rabat, Morocco

Mohamed Cherkaoui
Mohammed V University in Rabat
Rabat, Morocco

Kamal Elyalaoui
Mohammed V University in Rabat
Rabat, Morocco

Mohammed Ouassaid 
Mohammed V University in Rabat
Rabat, Morocco

ISSN 2198-4182

Studies in Systems, Decision and Control

ISBN 978-3-030-98736-7

<https://doi.org/10.1007/978-3-030-98737-4>

ISSN 2198-4190 (electronic)

ISBN 978-3-030-98737-4 (eBook)

© The Editor(s) (if applicable) and The Author(s), under exclusive license to Springer Nature Switzerland AG 2022

This work is subject to copyright. All rights are solely and exclusively licensed by the Publisher, whether the whole or part of the material is concerned, specifically the rights of translation, reprinting, reuse of illustrations, recitation, broadcasting, reproduction on microfilms or in any other physical way, and transmission or information storage and retrieval, electronic adaptation, computer software, or by similar or dissimilar methodology now known or hereafter developed.

The use of general descriptive names, registered names, trademarks, service marks, etc. in this publication does not imply, even in the absence of a specific statement, that such names are exempt from the relevant protective laws and regulations and therefore free for general use.

The publisher, the authors and the editors are safe to assume that the advice and information in this book are believed to be true and accurate at the date of publication. Neither the publisher nor the authors or the editors give a warranty, expressed or implied, with respect to the material contained herein or for any errors or omissions that may have been made. The publisher remains neutral with regard to jurisdictional claims in published maps and institutional affiliations.

This Springer imprint is published by the registered company Springer Nature Switzerland AG
The registered company address is: Gewerbestrasse 11, 6330 Cham, Switzerland

Preface

The present book *Modeling, Optimization and Intelligent Control Techniques in Renewable Energy Systems—An Optimal Integration Of Renewable Energy Resources Into Grid* publishes a good work in the field of renewable energy and control, presented in an informal and high-quality manner. The book's content is fascinating and appealing because it covers a wide range of technologies and control techniques, such as advanced robust control, intelligent control methods, wind farm, fractional-order controllers, algorithm optimizations, PV-CSP hybridization, thermal energy storage, dispatching strategy, modeling, mono-objective optimization and multi-objective optimization.

The goal is to include the theory, applications and perspectives on current and future advancements in renewable energy control and optimization, variable converters and related domains, as well as the paradigms and methodologies that underpin them.

The chapters in this book are written for graduate students, researchers, educators, engineers and scientists who need to know about mathematical analysis theories, methods and applications.

This book provides two parts. It has a total of 11 chapters, which are organized as follows: the first part focuses on applications of control theory on wind turbine and comprises six chapters.

The chapter *Introduction to Power System Stability and Wind Energy Conversion System* discusses the power system stability and the identification of the many forms and causes of instabilities in the power system such as voltage and frequency instability, as well as the frequency control types and the active power management capability constraints. The description of the grid code requirements for integration of wind energy conversion system into grid will be presented.

The chapter *Description and Modeling of Wind Energy Conversion System* presents the modeling of the different elements of the variable speed wind power system based on a squirrel cage induction generator, as well as modeling of grid, filters, transformer and transmission line. The infinite grid model, dynamic grid model, RL filter model and LCL filter model are considered. These models are developed in the (d, q) reference frame, using the Park transformation.

The chapter *Power Quality Improvement of Wind Energy Conversion System Using a Fuzzy Nonlinear Controller* proposes a fuzzy sliding mode control (Fuzzy-SMC) using a smooth function based on fuzzy logic. The proposed control algorithm is used to control the wind energy conversion system connected into the grid through a LCL filter with passive damping and to reduce the harmonics due to the chattering phenomenon. The proposed control system is validated by the numerical simulation and also validated experimentally using a test bench based on DSPace Board and three-phase inverter.

The chapter *Supervisory and Power Control Systems of a WF for Participating in Auxiliary Services* investigates a fuzzy PIFPI controller for reactive power and LVRT control in an uncompensated power system. The supervision system based on proportional distribution algorithm, according to three operating modes (MPPT control mode, PQ control mode and fault control mode) is developed to ensure the optimal operation of grid-connected wind farm based on the squirrel cage induction generator.

The chapter *LVRT Control Using an Optimized Fractional Order Fuzzy Controller of a Wind Farm* proposes the fractional order fuzzy controller (FOPI-Fuzzy-FOPI) to improve the voltage and reactive power responses and studies the problem of voltage drop in an uncompensated power system. The supervisory system ensures the cooperation between the different parts of the wind farm system and the optimal interaction between the wind turbines.

The chapter *Primary Frequency Control for Wind Farm Using a Novel PI Fuzzy PI Controller* addresses the participation of the wind farm in primary frequency control using inertial power reserve supported by pitch control strategy. The proposed PI-Fuzzy-PI (PIFPI) controller for primary frequency control ensures the balance between power demand and power production, provides high performance and satisfies the grid code requirements. The WF of 90 MW capacity is aggregated into a multi-machine model. It consists of 3 equivalent wind turbines based on squirrel cage induction generator and is connected to two grid areas.

The second part of this book includes five chapters and emphasis on the modeling and optimization of hybrid photovoltaic (PV)-concentrated solar power (CSP) systems coupled to a thermal energy storage system.

The chapter *Hybridization PV-CSP: An Overview* investigates an overview of hybrid photovoltaic (PV)-concentrated solar power (CSP) system. The challenges that can be addressed based on the world energy context are presented. In this context, renewable energy sources are presented as an ecological and economical alternative to fossil energies for the production of electricity. Then, the issues and proposed solution related to the grid integration of renewable energy sources are discussed. Finally, a survey of the literature on hybridization PV-CSP is presented.

The chapter *Detailed Modeling of Hybrid PV-CSP Plant* focuses on modeling of hybrid PV-CSP systems. Firstly, the mathematical model is presented to calculate the hourly electrical power produced by the PV plant and the hourly electrical power generated by the solar field of the CSP plant based on parabolic trough technology. Finally, a dispatch strategy is proposed in order to manage the power flows in the hybrid PV-CSP system to supply the requested load.

The chapter *Techno-economic Parametric Study of Hybrid PV-CSP Power* proposes a parametric study of three main solar plants (PV, CSP and hybrid PV-CSP). This study focuses on evaluating the influence of decision parameters (PV orientation angles, solar multiple (SM), thermal energy storage capacity (TES) and fraction of hybridization) on solar power plants, by calculating the electrical annual energy and electricity cost. Several simulations have been established and discussed in detail to evaluate the optimal configuration of the PV-CSP in comparison with PV plant and CSP plant.

The chapter *Optimal PV-CSP System Sizing Using Mono Objective Optimisation* addresses a mono objective optimization model to find the optimum size of hybrid PV-CSP plant so as to meet the requested load with possible minimum electricity cost and highest efficiency. Hybrid particle swarm optimization (PSO)–Cuckoo search (CS) algorithm have been used through this model for determining the optimum size of the PV-CSP system, and the minimum electricity cost at a pre-determined level of capacity factor value, in order to satisfy two types of requested load.

The chapter *The Multi-objective Optimization of PV-CSP Hybrid System with Electric Heater* presents a multi-objective optimization approach of the hybrid PV-CSP system coupled to an electric heater (EH), which is used to convert the excess electrical energy from the PV plant into thermal energy that will be stored for later use. Therefore, a model of the PV-CSP-EH plant was established and a multi-objective optimization using the genetic algorithm was adopted. The purpose of the optimization is to minimize the electricity cost and dumped energy and to maximize the capacity factor simultaneously. The Final optimal configurations are obtained from the Pareto front by applying a decision-making method.

Valenciennes, France
Rabat, Morocco
Rabat, Morocco
Rabat, Morocco
Rabat, Morocco
December 2021

Moussa Labbadi
Kamal Elyaalaoui
Loubna Bousselamti
Mohammed Ouassaid
Mohamed Cherkaoui

Acknowledgements

My special thanks go to my parents, my brother and my friends for their moral and encouragement.

Valenciennes, France

Moussa Labbadi

My special thanks go to all members of my family, my father Mohamed Elyaalaoui, who passed away too early, my mother, my friends for their support and baby Joudi, who was born at the same time as this book.

Rabat, Morocco

Kamal Elyaalaoui

Thanks first and last to Allah for the utmost help and support during this work. Thanks to my parents, my sisters, my brother and my friends, without their support and most of all love, the completion of this work would not have been possible.

Rabat, Morocco

Loubna Bousselamti

Contents

Part I Intelligent Control on Wind Farm

| | | |
|----------|--|-----------|
| 1 | Introduction to Power System Stability and Wind Energy Conversion System | 3 |
| 1.1 | Introduction | 3 |
| 1.2 | Stability of the Electrical Power System | 4 |
| 1.3 | Power System Stability and Wind Energy Conversion System | 4 |
| 1.4 | Voltage Dips and Grid Code Requirements | 5 |
| 1.4.1 | Voltage Stability | 6 |
| 1.4.2 | Types of Voltage Stability | 6 |
| 1.4.3 | Main Causes of Voltage Instability | 7 |
| 1.4.4 | Grid Code Requirements for Voltage Dip | 8 |
| 1.5 | Frequency Stability and Grid Code Requirements | 8 |
| 1.5.1 | Main Causes of Frequency Instability | 9 |
| 1.5.2 | Example of Frequency Instability | 10 |
| 1.5.3 | Grid Code Requirements | 12 |
| 1.5.4 | Frequency Control | 13 |
| 1.6 | Conclusion | 15 |
| | References | 16 |
| 2 | Description and Modeling of Wind Energy Conversion System | 19 |
| 2.1 | Introduction | 19 |
| 2.2 | Wind Turbine | 20 |
| 2.2.1 | Modeling of Turbine in Per Unit Notation | 20 |
| 2.2.2 | Modeling of the Shaft in Per-unit System | 22 |
| 2.3 | Modeling of the Squirrel-Cage Asynchronous Generator in the Park Reference Frame | 22 |
| 2.3.1 | Modeling of SCIG in the Park Reference Frame | 23 |
| 2.3.2 | Electrical Equations of Generator in Park Reference Frame | 23 |

| | | |
|----------|--|-----------|
| 2.3.3 | Per-unit System for Modeling | 23 |
| 2.3.4 | Electromagnetic Torque and Power | 25 |
| 2.4 | Modeling of the RL Filter in pu System | 26 |
| 2.5 | Modeling of Transformer and Transmission Line | 27 |
| 2.5.1 | Transformer Model | 27 |
| 2.5.2 | Transmission Line Model | 28 |
| 2.6 | Modeling of the LCL Filter | 28 |
| 2.6.1 | Model of LCL Filter in (abc) Reference Frame | 29 |
| 2.6.2 | Model of LCL Filter in Park Reference Frame | 30 |
| 2.7 | Electrical Power Network | 31 |
| 2.7.1 | Infinite Grid Model | 31 |
| 2.7.2 | Dynamic Model of Grid | 31 |
| 2.8 | Conclusion | 32 |
| | References | 32 |
| 3 | Power Quality Improvement of Wind Energy Conversion System Using a Fuzzy Nonlinear Controller | 35 |
| 3.1 | Introduction | 35 |
| 3.2 | Modeling of Grid-Side System | 35 |
| 3.2.1 | Modeling of DC Bus | 35 |
| 3.2.2 | Model of Filter | 38 |
| 3.3 | SMC of Grid-Side Converter | 39 |
| 3.3.1 | SMC of Grid-Side Current | 39 |
| 3.3.2 | Analysis of System Stability | 41 |
| 3.3.3 | Sliding Mode Control of Grid Current Without RC Sensor | 43 |
| 3.3.4 | Fuzzy Smooth Function of FSMC | 43 |
| 3.3.5 | FSMC Stability Analysis | 44 |
| 3.4 | Simulation Validation | 46 |
| 3.4.1 | Comparative Study of Filters and Their Control Systems | 46 |
| 3.4.2 | Robustness Test Against Variation of Parameters | 49 |
| 3.5 | Experimental Validation Approach | 52 |
| 3.5.1 | Comparative Study Between RL Filter and LCL Filter | 52 |
| 3.5.2 | Comparative Study for Control Methods Using LCL Filter | 53 |
| 3.5.3 | Robustness Test | 54 |
| 3.6 | Conclusion | 55 |
| | References | 61 |

| | | |
|----------|--|-----------|
| 4 | Supervisory and Power Control Systems of a WF for Participating in Auxiliary Services | 63 |
| 4.1 | Introduction | 63 |
| 4.2 | Wind Farm Supervision System | 64 |
| 4.2.1 | Power Dispatching Using Proportional Distribution Algorithm | 64 |
| 4.2.2 | Supervisory System Configuration | 65 |
| 4.3 | Transient Control Modes of Wind Turbines | 69 |
| 4.3.1 | MPPT Control Mode | 69 |
| 4.3.2 | PQ Control Mode | 69 |
| 4.3.3 | Fault Control Mode | 70 |
| 4.3.4 | Validation and Discussion | 71 |
| 4.4 | Fault Control Strategy Using Hierarchical Fuzzy Controller | 77 |
| 4.4.1 | Dynamic Model of Grid for Voltage-Reactive Power Control | 77 |
| 4.4.2 | Voltage Control at PCC | 79 |
| 4.4.3 | Proposed Fuzzy Hierarchical Controller | 80 |
| 4.4.4 | Validation and Discussion | 82 |
| 4.5 | Conclusion | 85 |
| | References | 86 |
| 5 | LVRT Control Using an Optimized Fractional Order Fuzzy Controller of a Wind Farm | 87 |
| 5.1 | Introduction | 87 |
| 5.2 | Wind Farm Management According to Grid Code Recommendations | 88 |
| 5.2.1 | Central Supervision Unit | 88 |
| 5.2.2 | Local Supervision Unit | 88 |
| 5.2.3 | System Protection | 89 |
| 5.3 | Power System Modeling | 89 |
| 5.3.1 | Objectives of the Study and Choice of Model Type | 89 |
| 5.4 | Wind Farm Management According to Grid Code Requirements | 91 |
| 5.4.1 | Grid Code Requirements | 91 |
| 5.5 | Proposed Fault Control Strategy | 92 |
| 5.5.1 | Voltage Control | 92 |
| 5.5.2 | Design of Fractional Order PIFO-Fuzzy-PIFO Controller | 92 |
| 5.5.3 | Fractional Order Preliminaries | 94 |
| 5.5.4 | Proposed FOPI-Fuzzy-FOPI Fractional Order Controller | 95 |

| | | |
|---|---|------------|
| 5.6 | Validation and Discussion | 96 |
| 5.6.1 | Comparative Study of Voltage and Reactive Power Responses | 98 |
| 5.6.2 | Performance of the Supervision System | 101 |
| 5.7 | Conclusion | 104 |
| | References | 105 |
| 6 | Primary Frequency Control for Wind Farm Using a Novel PI Fuzzy PI Controller | 107 |
| 6.1 | Introduction | 107 |
| 6.2 | Aggregate Model for Frequency-Power Response Study | 108 |
| 6.2.1 | Aggregate Model of the Wind Farm | 108 |
| 6.2.2 | Equivalent Parameters of Aggregated Model | 111 |
| 6.2.3 | Power System Model for Frequency Control | 111 |
| 6.2.4 | Adaptation of Power System Model to Grid Code Recommendations | 115 |
| 6.3 | Proposed Hierarchical Fuzzy Logic Controller for Primary Frequency Control | 116 |
| 6.3.1 | Power Reserve Control | 116 |
| 6.3.2 | Frequency Control | 118 |
| 6.4 | Simulation Results and Discussion | 121 |
| 6.4.1 | Comparative Study of the Frequency and Power Responses | 121 |
| 6.4.2 | Dynamic Behavior of WTs | 122 |
| 6.5 | Conclusion | 125 |
| | References | 125 |
| Part II Modeling, Optimization and Sizing of Hybrid PV-CSP Plants PV-CSP Hybrid Plants | | |
| 7 | Hybridization PV-CSP: An Overview | 129 |
| 7.1 | Introduction | 129 |
| 7.2 | Global Energy Context | 129 |
| 7.3 | Renewable Energies Sources (RES) | 131 |
| 7.3.1 | The Context of Integration of Renewable Energies Sources in the Electrical Grid | 131 |
| 7.3.2 | Issues Related to the Integration of Renewable Energies Sources | 131 |
| 7.3.3 | Proposed Solutions | 132 |
| 7.4 | Solar Energy | 133 |
| 7.5 | Hybrid Energy Systems (HES) | 133 |
| 7.5.1 | PV Hybrid Systems | 134 |
| 7.5.2 | CSP Hybrid Systems | 135 |

| | | |
|-----------|---|------------|
| 7.6 | PV-CSP Hybridization | 136 |
| 7.7 | Literature Review on PV-CSP Hybridization | 137 |
| 7.8 | Conclusion | 140 |
| | References | 140 |
| 8 | Detailed Modeling of Hybrid PV-CSP Plant | 145 |
| 8.1 | Introduction | 145 |
| 8.2 | Solar Position | 145 |
| 8.3 | PV Model | 148 |
| 8.4 | CSP Model | 153 |
| 8.5 | Dispatch Strategy | 161 |
| 8.6 | Conclusion | 161 |
| | References | 162 |
| 9 | Techno-economic Parametric Study of Hybrid PV-CSP Power Plants | 165 |
| 9.1 | Introduction | 165 |
| 9.2 | Technical and Economic Assessment | 165 |
| | 9.2.1 Technical Assessment | 166 |
| | 9.2.2 Economic Assessment | 166 |
| 9.3 | Site Selection | 168 |
| 9.4 | Parametric Study of Solar Power Plants | 168 |
| | 9.4.1 The PV Plant | 168 |
| | 9.4.2 The CSP Plant | 172 |
| | 9.4.3 The Hybrid PV-CSP Plant | 175 |
| 9.5 | Findings | 179 |
| 9.6 | Conclusion | 180 |
| | References | 180 |
| 10 | Optimal PV-CSP System Sizing Using Mono Objective Optimisation | 183 |
| 10.1 | Introduction | 183 |
| 10.2 | Optimization Problem Statement | 183 |
| | 10.2.1 Objective Function | 183 |
| | 10.2.2 Constraint | 184 |
| | 10.2.3 Decision Variables | 184 |
| 10.3 | Optimization Algorithm | 184 |
| 10.4 | Result and Discussion | 188 |
| | 10.4.1 Case 1 | 188 |
| | 10.4.2 Case 2 | 190 |
| | 10.4.3 Comparative Study (A PV-CSP Plant and a CSP Plant) | 190 |
| 10.5 | Conclusions | 192 |
| | References | 192 |

| | | |
|--|--|-----|
| 11 | The Multi-objective Optimization of PV-CSP Hybrid System with Electric Heater | 195 |
| 11.1 | Introduction | 195 |
| 11.2 | Literature Review | 195 |
| 11.3 | System Modeling | 197 |
| 11.4 | Optimization Problem Statement | 198 |
| 11.5 | Multi-objective Optimization Algorithm | 198 |
| 11.6 | Multi-criteria Decision-Making Method | 199 |
| 11.7 | Results and Discussion | 201 |
| 11.8 | Conclusions | 206 |
| | References | 206 |
| 12 | Summary and Scope | 209 |
| 12.1 | Summary of Full Text | 209 |
| 12.2 | Future Research Prospect | 211 |
| Appendix A: Part I: Parameters and Preliminaries of Wind Energy Conversion System and Controllers | | 213 |
| Appendix B: Part II: Technical and Economic Parameters of PV and CSP Plants | | 223 |

Abbreviations

| | |
|-----------------|---|
| ADC | Analog-to-digital converter |
| AESO | Alberta Electric System Operator |
| CF | Capacity factor |
| CRPC | Constant Reactive Power Control |
| CSP | Concentrated solar power |
| DAC | Digital-to-analog converter |
| DFIG | Double-Fed Asynchronous Generator |
| EES | Electrical energy storage |
| EH | Electric heater |
| ENTSO-E | The European Network of Transmission System Operators for Electricity |
| FAM | Full Aggregated Model |
| FLC | Fuzzy Logic Controller |
| FO | Fractional Order |
| FOC | Fractional Order Controller |
| FOPI-fuzzy-FOPI | Fractional-order PI Fuzzy PI controller |
| Fuzzy-SMC | Fuzzy Sliding Mode Control |
| GCR | Grid Code Requirements |
| HES | Hybrid energy systems |
| HFC | Hierarchical Fuzzy Controller |
| HRES | Hybrid renewable energy system |
| IEA | International energy agency |
| IEC | International Electrotechnical Commission |
| LCOE | Levelized cost of electricity |
| LFSM | Limited Frequency Sensitive Mode |
| LFSM-U | Limited Frequency Sensitive Mode under-frequency |
| LVRT | Low Voltage Ride through |
| MMM | Multi-Machine Model |
| MPPT | Maximum Power Point Tracking |
| ONEE | Office National of Electricity |

| | |
|------------|---|
| PB | Power block |
| PCC | Point of Common Coupling |
| PDA | Proportional Distribution Algorithm |
| PDF | PD-Fuzzy controller |
| PFC | Primary frequency control |
| PID | Proportional–Integral–Derivative |
| PIF | PI-Fuzzy controller |
| PIFPI | PI-Fuzzy-PI |
| PMSG | Permanent Magnet Synchronous Generator |
| PQ control | Active and reactive powers control |
| PSOA | Particle Swarm Optimization Algorithm |
| PV | Photovoltaic |
| PWM | Pulse-Width Modulation |
| SAM | Semi-Aggregated Model |
| SCIG | Squirrel Cage Induction Generator |
| SF | Solar field |
| SG | Synchronous Generator |
| SMC | Sliding Mode Control |
| TES | Thermal energy storage |
| THD | Total Harmonic Distortion |
| TSO | Transmission System Operator |
| UCTE | Union for Coordination of Transmission of Electricity |
| WPP | Wind Power Plant |

Acronyms

System Variables

| | |
|---------------|---|
| λ | The speed ratio |
| β | The blade orientation angle |
| V_{base} | Base voltage |
| $V_{nominal}$ | Nominal voltage |
| P_{base} | Base power |
| $P_{nominal}$ | Nominal power |
| C_{em} | Electromagnetic torque developed by the generator |
| s | Is the Laplace operator |
| V_{sd} | d-axis component of stator voltage |
| V_{sq} | q-axis component of stator voltage |
| V_{rd} | d-axis component of rotor voltage |
| V_{rq} | q-axis component of rotor voltage |
| i_{sd} | d-axis component of stator current |
| i_{sq} | q-axis component of stator current |
| i_{rd} | d-axis component of rotor current |
| i_{rq} | q-axis component of rotor current |
| ω_s | Stator frequency |
| ω_g | Grid frequency |
| P | Active power |
| Q | Reactive power |
| ϕ_{sq} | d-axis component of stator flux |
| ϕ_{sd} | q-axis component of stator flux |
| ϕ_{rq} | d-axis component of rotor flux |
| ϕ_{rd} | q-axis component of rotor flux |
| v_1 | Voltages at the output of the filter |
| v_2 | Voltages at the output of the transformer |

| | |
|----------|--|
| v_g | Voltages at PCC |
| i_f | Current flowing through the filter |
| v_{1d} | d-axis components of grid voltage |
| v_{1q} | q-axis components of grid voltage |
| v_{md} | d-axis components of voltage at the converter output |
| v_{mq} | q-axis components of voltage at the converter output |
| u_I | Voltages at the filter input |
| u_G | Voltages at the filter output |

Parameters

| | |
|------------|-----------------------------------|
| H_p | Blade inertia constant |
| H_h | Inertia constant of the hub |
| H_g | Inertia constant of the generator |
| f | Coefficient of friction in “pu” |
| R_s | Stator resistance |
| R_r | Rotor resistance |
| l_s | Stator leakage inductance |
| l_r | Rotor leakage inductance |
| L_m | Mutual inductance |
| R_f | RL filter resistance |
| L_f | RL filter inductance |
| R_F | LCL filter resistance |
| C_F | LCL filter capacitance |
| R_{RL} | RL filter resistance |
| L_{RL} | RL filter inductance |
| R_{on} | Internal resistance |
| R_{snub} | Snubber resistance |
| T_f | The fall time |
| T_t | Tail time |
| V_f | Forward voltage |
| R_{ca} | Resistance of line and cable |
| L_{ca} | Inductance of line and cable |
| C_{ca} | Capacitor of line and cable |
| R_{tr} | Resistance of transformer |
| L_{tr} | Inductance of transformer |
| R_f | Resistance of filter |
| L_f | Inductance of filter |
| Tr | Low-pass filter time constant |
| $[Ka, Ta]$ | Regulator gain & time constant |

| | |
|-----------------------------|--|
| $[K_e, T_e]$ | Exciter |
| $[T_b, T_c]$ | Transient gain reduction |
| $[K_f, T_f]$ | Damping filter gain & time constant |
| $[E_{fmin}, E_{fmax}, K_p]$ | Regulator output limits and gain |
| $[V_{t0}(pu), V_{f0}(pu)]$ | Initial values of terminal voltage and forward voltage |
| P_{tr} | Transformer nominal power |
| R_f | R_L Filter resistance |
| L_f | R_L Filter inductance |
| R_{1-eq} | Resistance of primary of the transformer |
| R_{2-eq} | Resistance of secondary of the transformer |
| L_{1-eq} | Inductance of primary of transformer |
| L_{2-eq} | Inductance of secondary of transformer |
| R_{L-eq} | Resistance of PI section line |
| L_{L-eq} | Inductance of PI section line |
| C_{L-eq} | Capacitor value of PI section line |
| D | Load damping coefficient |
| R | Droop referred to percent speed regulator |
| ω_0 | Rated rotor speed |
| V_n | Rated voltage (RMS Ph-Ph) |
| H_G | Inertia constant of the grid generator |
| T_G | Governor time constant |
| T_{CH} | Turbine time constant |
| L_i | Inductance of converter side |
| L_g | Grid side inductance |
| C_f | The filter capacitor |
| R_f | The damping resistor |
| δ_s | Solar declination |
| ω_s | Hour angle |
| α_s | Solar altitude |
| θ_z | Zenith angle |
| γ_s | Solar azimuth |
| ϕ_s | Latitude |
| λ_s | Longitude |
| d | Number of the day |
| E_{time} | Equation of time |
| Tz | Time zone |
| γ | Azimuth angle |
| i | Tilt angle |
| θ_{PV} | Incidence angle for PV module |
| G_{tilted} | Global tilted irradiance |
| B_{tilted} | Beam tilted irradiance |
| D_{tilted} | Diffuse tilted irradiance |
| R_{tilted} | Reflected irradiance |
| B_n | Direct normal irradiance |

| | |
|---------------------|--|
| G_h | Global horizontal irradiance |
| D_h | Diffuse horizontal irradiance |
| ρ | Albedo |
| P_{DC} | Power output generated by solar PV field |
| A_{ref} | Area of PV module |
| N_{module} | Number of modules |
| η_{module} | PV module efficiency |
| $T_{module,ref}$ | PV module temperature under standard test conditions |
| $\eta_{module,ref}$ | PV module efficiency under standard test conditions |
| γ_f | Power temperature coefficient |
| T_c | PV cell temperature |
| T_{amb} | Ambient temperature |
| V_{wind} | Wind velocity |
| $\eta_{inverter}$ | Inverter efficiency |
| f_{losses} | Factor losses |
| $P_{el,pv}$ | Output power of a PV system |
| P_{pv} | PV installed capacity |
| $p_{th,incident}$ | Thermal power incident on the solar field |
| A_{field} | Solar field's area |
| $p_{th,absorbed}$ | Thermal power absorbed by the solar field |
| η_{sf} | Field efficiency |
| θ_{csp} | Incidence angle for solar collector |
| η_{shadow} | Shading losses |
| η_{end} | End losses |
| $L_{spacing}$ | Spacing between the collector's rows |
| A_{col} | Width of the collector |
| L_{col} | Length of the collector |
| L_{focal} | Focal length of the solar collector |
| η_{col} | Collector efficiency |
| η_{rec} | Receiver efficiency |
| P_{CSP} | CSP installed capacity |
| η_{pb} | Power block efficiency |
| SM | Solar multiple |
| $p_{th,losses}$ | Heat losses |
| $p_{th,rec}$ | Receiver losses |
| $p_{th,pipe}$ | Pipe system losses |
| $T^{sf,in}$ | Inlet temperature |
| $T^{sf,out}$ | Outlet temperature |
| C_{tes} | System storage capacity |
| h_{tes} | Storage duration |

List of Figures

| | | |
|-----------|--|----|
| Fig. 1.1 | Stability classification of the electrical power system | 5 |
| Fig. 1.2 | Simplified equivalent scheme of transmission line | 7 |
| Fig. 1.3 | German grid code requirements: a Fault voltage profile, b Curve of reactive current versus voltage drop for Voltage control by the reactive current injection [31] | 9 |
| Fig. 1.4 | Map of the UCTE area divided into three zones [36] | 11 |
| Fig. 1.5 | Frequency records until the splitting of a zone (area splitting) [36] | 11 |
| Fig. 1.6 | Frequency records after the division of the zones [36] | 12 |
| Fig. 1.7 | Electrical interconnections between Morocco and its neighbor countries [37] | 12 |
| Fig. 1.8 | ENTSO-E grid code requirements, a Active power response characteristics versus frequency deviation, b Activation time of active power frequency response | 13 |
| Fig. 1.9 | Schematic of the frequency control type with activation periods, after power imbalance | 14 |
| Fig. 1.10 | Active power management capability constraints | 15 |
| Fig. 2.1 | Structure of the wind turbine generator. | 20 |
| Fig. 2.2 | Turbine model implemented in MATLAB/Simulink. | 21 |
| Fig. 2.3 | Curves of the power coefficient $C_p(\lambda, \beta)$: a for different values of β and b $C_p(\lambda, \beta)$ versus λ and β | 21 |
| Fig. 2.4 | Shaft and wind turbine model. | 22 |
| Fig. 2.5 | Block diagram of the generator model | 25 |
| Fig. 2.6 | Scheme of the electrical system linking source to the grid | 26 |
| Fig. 2.7 | Equivalent simplified electrical scheme of a single phase of the transformer brought back to the primary. | 27 |
| Fig. 2.8 | Electrical scheme of the three-phase transmission line | 28 |
| Fig. 2.9 | Electrical scheme of filter, transformer and transmission line | 28 |

| | | |
|-----------|--|----|
| Fig. 2.10 | a Single-phase equivalent scheme of the LCL filter and b Model block of the LCL filter | 30 |
| Fig. 2.11 | Single-phase electrical scheme of the infinite power network with short-circuit impedance | 31 |
| Fig. 2.12 | Synoptic scheme of the power network with the possibility of parameterization for participation in the auxiliary service. | 32 |
| Fig. 3.1 | Block diagram of the studied system with LCL filter and converter control | 36 |
| Fig. 3.2 | The Gaussian membership functions: a Input membership functions b Output membership functions and c Surface of output versus input. | 45 |
| Fig. 3.3 | Modeling scheme in MATLAB/Simulink used to obtain the simulation results | 47 |
| Fig. 3.4 | Simulation results of SMC using LCL filter and without RC sensor | 47 |
| Fig. 3.5 | The simulation results of SMC with the LCL filter and the use of sensors at the RC branch. a THD of the current, b Power and DC bus voltage and c Current passing through RC branch of the filter | 48 |
| Fig. 3.6 | Simulation results of SMC with the RL filter without taking into account the power loss: a current THDi and b Power and voltage of DC bus | 48 |
| Fig. 3.7 | Simulation results of SMC used for current control with the RL filter and the PI controller used for V_{dc} control: a current THDi and b Power and voltage of DC bus | 49 |
| Fig. 3.8 | Simulation results of SMC for RL filter taking into account power loss: a THD of the current and b Power and voltage of DC bus. | 50 |
| Fig. 3.9 | Simulation results of fuzzy SMC for the LCL filter taking into account the power loss and without using sensor in the RC branch: a THD of current and b Power and voltage of the DC bus | 50 |
| Fig. 3.10 | Simulation results of robustness test against parameter variation of -60% of DC bus capacitance value (using RL filter and SMC for current control). a DC bus voltage control using SMC and b V_{dc} voltage regulation using PI controller | 51 |
| Fig. 3.11 | Simulation results of robustness test of the proposed Fuzzy-SMC control against parameter variations of -60% : a variation of the LCL filter parameters and b variation of the DC bus capacitance value. | 51 |
| Fig. 3.12 | Synoptic diagram of the experimental platform. | 52 |
| Fig. 3.13 | Flow chart for coupling inverter to grid | 53 |

| | | |
|-----------|---|----|
| Fig. 3.14 | Experimental results of three phases at output of RL filter, a three-phase voltages, b three-phase currents, c THDv of voltage and d THDi of current. | 54 |
| Fig. 3.15 | Experimental results of three phases at output of LCL filter, a three-phase voltages, b three-phase currents, c THDv of voltage and d THDi of current. | 55 |
| Fig. 3.16 | Experimental results of SMC with LCL filter and RC sensor, a three-phase voltages, b three-phase currents c THDv with maximum values, d THDi with maximum values, e three-phase currents of RC branch and f currents of 'd' and 'q' axes of RC branch of LCL filter | 56 |
| Fig. 3.17 | Experimental results of the sliding mode control with LCL filter and without RC sensor, a Three-phase voltages, b Three-phase voltages c THDv with maximum values, d THDi with maximum values | 57 |
| Fig. 3.18 | Experimental results of the fuzzy sliding mode control with LCL filter and without RC sensor, a Three-phase voltages, b Three-phase currents, c THDv with maximum values, d THDi with maximum values | 58 |
| Fig. 3.19 | Experimental results of active power at the LCL filter output using: a Vector control, b Conventional SMC, c Fuzzy-SMC, and d SMC with RC sensor addition | 59 |
| Fig. 3.20 | The two circuits of the switching relays for connection to the grid and variation of the filter inductance | 60 |
| Fig. 3.21 | THD of current and voltage for robustness test of proposed Fuzzy-SMC during LCL filter inductance variation of -50% | 60 |
| Fig. 4.1 | Block diagram of the wind farm connected to the power network. | 64 |
| Fig. 4.2 | Diagram of the adopted proportional distribution algorithm | 66 |
| Fig. 4.3 | Schematic of the supervision system configuration | 67 |
| Fig. 4.4 | Overall diagram of wind farm and converter control | 70 |
| Fig. 4.5 | Global schematic of WF connected to the grid developed in MATLAB/Simulink | 72 |
| Fig. 4.6 | Simulation results for scenario 1: a Grid voltage, b Three wind profiles. | 73 |
| Fig. 4.7 | Simulation results for scenario 1: a Reactive current at PCC (pu), b Voltage V_{dc} of 1st wind turbine | 74 |
| Fig. 4.8 | Simulation results for scenario 1: Active and reactive powers of Wind farm | 74 |
| Fig. 4.9 | Simulation results for scenario 1: a 1st wind turbine power, b 2nd wind turbine power and c 3rd wind turbine power | 75 |

| | | |
|-----------|---|----|
| Fig. 4.10 | Simulation results for scenario 2: PQ control from 0 to 6 s, MPPT control from 6 to 12 s and voltage drop from 80% to 9 s: a grid voltage, b the three wind profiles | 76 |
| Fig. 4.11 | Simulation results for scenario 2: PQ control from 0 to 6 s, MPPT control from 6 to 12 s and voltage drop from 80% to 9 s: a Reactive current at PCC (pu), b current at PCC (pu) | 77 |
| Fig. 4.12 | Active and reactive power at PCC for scenario 2: a wind farm and b 1 st wind turbine | 78 |
| Fig. 4.13 | Active and reactive power at PCC for scenario 2: a 2 nd wind turbine wind turbine and b the 3 rd wind turbine | 79 |
| Fig. 4.14 | Overall structure of the test system of the electrical power network with the possibility of parameterization of voltage-reactive power control $Q(V)$ of the power network. | 80 |
| Fig. 4.15 | The proposed control strategy: a Schematic of the voltage control at the PCC and references for the active and reactive power generation, b Block diagram of the hierarchical PIFPI controller. | 81 |
| Fig. 4.16 | Shapes of fuzzy membership functions: a Input variables, b Output variable | 82 |
| Fig. 4.17 | Reactive power and voltage response for different controllers: a voltage at PCC, b reactive power response | 83 |
| Fig. 4.18 | Reactive power and voltage response for different controllers: a active power response, b zoom of active power response | 84 |
| Fig. 5.1 | Structures of the configured supervisory system and its main units | 89 |
| Fig. 5.2 | The block diagram of the dynamic power system test $Q(V)$ for voltage control through reactive power injection. | 91 |
| Fig. 5.3 | Proposed control system: a Diagram block for power references generation according to the three operating modes, b Design layout of fractional order PIFO-Fuzzy-PIFO controller with PSO parameter optimization | 93 |
| Fig. 5.4 | Flowchart of PSO algorithm for optimization the fractional order operators using Matlab/Simulink model. | 94 |
| Fig. 5.5 | The impact of fractional order parameter λ on the voltage response | 97 |
| Fig. 5.6 | Simulation results of different reactive power and voltage controllers: a voltage at the PCC, b reactive power response | 98 |
| Fig. 5.7 | Simulation results of the different reactive power and voltage controllers: a active power response, b zoom of the active power response | 99 |

| | | |
|-----------|---|-----|
| Fig. 5.8 | Simulation results of a scenario that includes PQ control [2, 6s], MPPT control [6, 10s] and voltage fault control activated at time 9 s. a PCC voltage, b the three wind profiles. | 101 |
| Fig. 5.9 | Simulation results of a scenario that includes PQ control [2, 6s], MPPT control [6, 10s] and voltage fault control activated at time 9 s. a Active power b Reactive power. | 102 |
| Fig. 5.10 | Simulation results of a scenario including PQ control [2, 6s], MPPT control [6, 10s] and voltage fault control activated at time 9 s. a PCC current, b the DC bus voltages of the 3 WTs | 103 |
| Fig. 6.1 | Model of the wind farm as a cluster of 30 wind turbines. | 108 |
| Fig. 6.2 | Aggregate models of the wind farm | 109 |
| Fig. 6.3 | Overall diagram of the farm connected to the electrical grid. | 110 |
| Fig. 6.4 | Turbine connected to a synchronous generator supplying an isolated load. | 112 |
| Fig. 6.5 | Transfer function relating speed and torques. | 112 |
| Fig. 6.6 | Transfer function linking mechanical speed and power in “per unit” notation | 113 |
| Fig. 6.7 | Global electrical grid diagram including generators and loads with the possibility to control the frequency and active power. | 114 |
| Fig. 6.8 | Ideal steady-state characteristics of a governor with speed droop | 115 |
| Fig. 6.9 | Power reserve control, a Optimal and deloaded power curves, b Block diagram for generating the pitch angle. Where T_β is the time constant of the pitch system servo motor. The speed and range of the pitch angle variation are set to $\pm 10^\circ/s$ and 0° to 90° , respectively | 117 |
| Fig. 6.10 | Generation of power and torque references for frequency control | 119 |
| Fig. 6.11 | Gaussian membership functions for the inputs and the output. | 119 |
| Fig. 6.12 | Block diagram of the proposed hierarchical fuzzy controllers: a PIFPI controller, b PDFPI controller | 120 |
| Fig. 6.13 | Block diagram of inertial controller for frequency control | 121 |
| Fig. 6.14 | Frequency responses (Hz) at the PCC: a using the five controllers, b their zoom. | 122 |
| Fig. 6.15 | The power response: a Active power (MW) and b Reactive power (MVAR) at PCC | 123 |
| Fig. 6.16 | Behaviours of the 3 WT-equs: a pitch angle response (degrees) and b active power response at the PCC (MW) | 124 |
| Fig. 6.17 | DC bus voltage responses of the three equivalent wind turbines | 124 |

| | | |
|-----------|---|-----|
| Fig. 7.1 | The breakdown of energy demand by source for the year 2020 [1] | 130 |
| Fig. 7.2 | Energy breakdown of world electricity production, 1971–2021 [1] | 131 |
| Fig. 7.3 | Applications of solar energy | 134 |
| Fig. 7.4 | PV-CSP hybridization scenarios | 137 |
| Fig. 8.1 | The annual variation of the solar declination (δ_s) | 147 |
| Fig. 8.2 | The annual variation of the equation of time (E_{time}) | 147 |
| Fig. 8.3 | Model of the PV plant | 149 |
| Fig. 8.4 | Model of the CSP plant | 154 |
| Fig. 8.5 | Solar field control Mode 1: HTF freeze protection, Mode 2: Warm-up and Mode 3: Normal operation. | 159 |
| Fig. 8.6 | Model of PV-CSP plant | 161 |
| Fig. 9.1 | a Annual DNI profile b Annual GHI profile. | 169 |
| Fig. 9.2 | Daily solarradiation (DNI and GHI) | 169 |
| Fig. 9.3 | The influence of varying the tilt and orientation angle on the annual energy produced bythe PV plant | 171 |
| Fig. 9.4 | The influence of varying tilt angle on the annual energy and the LCOE of the PV plant (for southern orientation) | 171 |
| Fig. 9.5 | The influence of TES size value on the CSP system energy produced: a TES = 6 h, b TES = 12 h (CSP plant with 100MW and SM = 3). | 173 |
| Fig. 9.6 | Variation of annual energy as function of TES size for different values of solar multiple. | 173 |
| Fig. 9.7 | Variation of LCOE as function of TES size for different values of solar multiple | 174 |
| Fig. 9.8 | The annual energy generated of all simulated scenarios | 176 |
| Fig. 9.9 | The LCOE of all simulated scenarios | 176 |
| Fig. 9.10 | The variation of electrical annual energy, capacity factor, and LCOE according to solar multiple for $h_{tes} = 12h$ | 178 |
| Fig. 10.1 | Load profiles. | 188 |
| Fig. 10.2 | The convergence of PSO-CS algorithm (Case 1, Load 1). | 189 |
| Fig. 10.3 | The convergence of PSO-CS algorithm (Load 2) | 191 |
| Fig. 11.1 | Simplified diagram of the PV-CSP-EH plant $P^{th,SF}$: Thermal power produced by solar field (CSP), $P^{SF,PB}$: Thermal power directly used by the power block from the solar field, $P^{to, TES}$: Thermal power sent to the TES, $P^{from, TES}$: Thermal power used by the power block from the TES system, P^{PV} : Electrical power produced by the PV plant, $P^{to, load}$: Electrical power directly used to satisfy the load from the PV, $P^{to, EH}$: the electrical power rejected by the PV plant and which will be sent to the EH, $P^{EH, TES}$: Dumped electrical powerand $P^{PV, CSP}$: Electrical power used to satisfy the load. | 197 |
| Fig. 11.2 | Pareto front obtained by optimization of the PV-CSP-EH | 201 |

| | | |
|-----------|---|-----|
| Fig. 11.3 | Pareto front in terms of PV installed capacity. | 202 |
| Fig. 11.4 | Pareto front in terms of CSP installed capacity. | 202 |
| Fig. 11.5 | Pareto front in terms of electric heater capacity | 203 |
| Fig. 11.6 | Pareto front in terms of solar multiple | 203 |
| Fig. 11.7 | Pareto front in terms of TES size | 204 |
| Fig. A.1 | The realised measurement circuits. | 219 |
| Fig. A.2 | Photo of the designed LCL filter | 220 |
| Fig. A.3 | SEMIKRON three-phase inverter and its connectors. | 221 |

List of Tables

| | | |
|------------|--|-----|
| Table 1.1 | Parameters for the complete activation of the active power range and the maximum allowable periods | 13 |
| Table 3.1 | Comparison between the performance of the filters and their proposed controls | 49 |
| Table 4.1 | Types of protection | 68 |
| Table 4.2 | Fuzzy logic rules for the voltage controller | 82 |
| Table 4.3 | Combination of voltage and reactive power controllers Reactive power controller | 84 |
| Table 5.1 | Fuzzy logic rules for the proposed controller the voltage controller | 96 |
| Table 5.2 | Combination of controllers for voltage and reactive power control | 100 |
| Table 6.1 | Fuzzy logic rules for primary frequency control | 120 |
| Table 6.2 | Frequency responses for an acceptable deviation from deadband of 0.01 Hz | 123 |
| Table 7.1 | PV-CSP projects around the world [43, 45–47]. | 137 |
| Table 9.1 | Simulated configurations | 175 |
| Table 10.1 | Mathematical test functions | 187 |
| Table 10.2 | Statistics for algorithms (PSO, CS et PSO-CS) | 187 |
| Table 10.3 | PSO-CS parameters | 188 |
| Table 10.4 | Optimization results (Load 1) | 190 |
| Table 10.5 | Optimization results (Load 2) | 191 |
| Table 10.6 | Optimization results for CSP plant alone (Load 1 and 2) | 191 |
| Table 11.1 | Optimization results (PV-CSP-EH power system) | 204 |
| Table 11.2 | Optimization results (PV-CSP power system) | 205 |
| Table A.1 | Parameters of the inverter, RL filter and LCL filter | 214 |
| Table A.2 | Control system parameters in per unit notation | 214 |
| Table A.3 | IEEE recommended practices and requirements for harmonic control in electrical power systems. | 215 |

| | | |
|------------|---|-----|
| Table A.4 | Limit values for harmonic voltage (MV, HV and EHV) | 215 |
| Table A.5 | Parameters of line, transformer and filter. | 215 |
| Table A.6 | Parameters of the excitation system. | 216 |
| Table A.7 | Parameters of the filter, transformer Tr1-1 and transmission line L1-1 | 216 |
| Table A.8 | Parameters of the grid synchronous generator | 217 |
| Table A.9 | Single phase parameters of the LCL filter | 218 |
| Table A.10 | The RL filter parameters of Single phase | 218 |
| Table B.1 | Technical parameters of the PV plant | 223 |
| Table B.2 | Economic parameters of the PV plant | 224 |
| Table B.3 | Technical parameters of the CSP plant | 224 |
| Table B.4 | Economic parameters of the PV plant | 225 |